Robotica (2023), **41**, pp. 566–586
doi:10.1017/S0263574722001436

RESEARCH ARTICLE

Cooperative control strategy of wheel-legged robot based on attitude balance

Yaojie Shen, Guangrong Chen*, Zhaoyang Li, Ningze Wei, Huafeng Lu, Qingyu Meng and Sheng Guo

Robotics Research Center, Beijing Jiaotong University, Beijing, 100044, P.R. China
*Corresponding author. E-mail: grchen@bjtu.edu.cn

Received: 28 May 2022; **Revised:** 29 August 2022; **Accepted:** 13 September 2022; **First published online:** 12 October 2022

Keywords: wheel-legged robot, cooperative control, control strategy, attitude balance, trajectory planning

Abstract
To integrate the uneven terrain adaptivity of legged robots and the fast capacity of wheeled robots on even terrains, a four wheel-legged robot is addressed and the cooperative control strategy of wheels and legs based on attitude balance is investigated. Firstly, the kinematics of wheel-legged robot is analyzed, which contains the legged and wheeled motion modal. Secondly, the cooperative control strategy of wheel-legged robot based on attitude balance is proposed. The attitude is calculated by using the quaternion method and complementary filtering, and the attitude stability control of the wheel-legged robot is studied. The trajectory planning of leg motion including walk and trot gait is implemented, and the differential control of wheeled motion is deduced. And then, the cooperative motion control of wheels and legs is achieved by keeping the attitude balance of robot body. Finally, a small prototype is set up to validate the feasibility and effectiveness of proposed method. The experimental results show that the established wheel-legged robot can do walk, trot, and wheel-leg compound motion to overcome many complex terrains and environments.

1. Introduction
Mobile robot is an automatic machine that is capable of locomotion and has the capability to move around in their environment and is not fixed to one physical location. Mobile robots have become more commonplace in commercial and industrial settings. Wheeled and legged robot are two classical kinds of mobile robot, and they are used in different applications [1, 2]. The wheeled robots can move very fast on flat grounds without too much body oscillation, but they cannot stride across some rough terrains. The legged robots can overcome very complex uneven terrains, but they cannot have the high speed and stability with wheeled robots [3]. This greatly limits the application and development of mobile robots [4].

In current years, many researchers and engineers want to seek for one kind of robot which own the advantages of wheeled and legged robots in one. As thus, the wheel-legged robot began to appear and developed rapidly. Jiehao Li *et al.* proposed a neural fuzzy-based model predictive tracking scheme (NFMPC) for reliable tracking control to the developed four wheel-legged robot, and the fuzzy neural network approximation is applied to estimate the unknown physical interaction and external dynamics of the robot system [5]. Zhihua Chen *et al*. provided a legged stable walking control strategy based on multi-sensor information feedback about BIT-NAZA-II, a large load parallel hexapod wheel-legged robot developing for the problem of vertical contact impact and horizontal sliding of heavy leg robot in complex terrain environments [6]. Shoukun Wang *et al.* proposed a whole-body control architecture includes the attitude controller, impedance controller, and center height controller that is developed for obstacle avoidance, which can ensure the horizontal stability of the body of the robot when it passes through obstacles in different terrain [7]. Xu Li *et al*. introduced the details of the wheel-legged robot (WLR), highlighting the innovative design and optimization of physical construction which is considered to maximize the mobile abilities, enhance the environmental adaptability, and improve the reliability of hydraulic system [8]. Hui Peng *et al.* designed a cooperative control framework to control attitude of a wheel-legged robot. And an impedance control based on force method and active disturbance rejection control (ADRC) are applied to improve the locomotion performance [9]. Kang Xu *et al*. proposed an adaptive variable impedance control (AVIC) method to minimize the force-tracking error for the forces of each leg that are exerted on the body, thereby maintaining a horizontal posture of the whole body and improving the stability [10]. Liwei Ni *et al*. studied the parameters uncertainty analysis of posture control of a four-wheel-legged robot with series slow active suspension system [11]. Fahad Raza *et al*. explored and analyzed the active arm control on top of the wheel-legged system to assist in its balance recovery during external pushes and disturbances and presentd a control framework to improve the stability and robustness of an underactuated self-balancing wheel-legged robot using its upper limb arm [12]. Shuai Wang *et al*. presented a balance control technique for a novel wheel-legged robot. To take into account nonlinearities of the model and obtain a large domain of stability, a nonlinear controller based on the interconnection and damping assignment - passivity-based control (IDA-PBC) method is exploited to control the robot in more general scenarios [13]. Leiei Cui *et al*. studied the adaptive optimal control problem for a wheel-legged robot in the absence of an accurate dynamic model. A crucial strategy is to exploit recent advances in reinforcement learning (RL) and adaptive dynamic programming (ADP) to derive a learning-based solution to adaptive optimal control [14]. Xi Chen *et al.* presented a novel approach to train action policies to acquire navigation skills for wheel-legged robots using deep reinforcement learning. The policy maps height-map image observations to motor commands to navigate to a target position while avoiding obstacles [15].

Even though there are many research about the configuration, control, and perception of wheeled-legged robot, the cooperation of wheels and legs is less discussed. Therefore, cooperative control strategy of wheel-legged robot based on attitude balance is proposed in this paper. The paper is organized as follows. In Section 2, the system model of wheel-legged robot is illustrated. In Section 3, the kinematics of wheel-legged robot is elaborated including wheeled and legged motion. In Section 4, the controller of wheel-legged robot is designed. In Section 5, experiments are implemented to validate the effectiveness and feasibility of proposed method. In Sections 6 and 7, discussions are taken and conclusions are drawn, respectively.

2. Model of wheel-legged robot

In this paper, a four wheel-legged robot, with wheel on the end effector of foot, is addressed. The robot is with 8 degree of freedoms (DoFs) in total and elbow-type leg structure, as shown in Fig. 1(a), where L is the length of robot body, W is the width of robot body, H is the height of the center of mass of robot, R_m is the radius of wheel, and l_1 and l_2 are the length of thigh and shank, respectively. The left front is the No. 1 leg, the right front is the No. 2 leg, the right rear is the No. 3 leg, and the left back is the No. 4 leg. The coordinates of center of gravity are $G = (G_x, G_z)$. p is the pitch angle of robot and r is the roll angle of robot. Noting that the wheel-legged robot is limited to move in the sagittal plane, since there does not exist extra DoF in legs for the lateral motion. Therefore, only a two-dimensional coordinates $O-XZ$ is set, and the coordinate y of center of gravity and the raw angle of robot are out of consideration. The robot assembly is shown in Fig. 1(b).

3. Kinematics of wheel-legged robot

The kinematics of wheel-legged robot contains legged [16] and wheeled [1] motion model.

3.1. Legged motion model

The single-leg structure of the wheel-legged robot is shown in Fig. 2. A plane coordinate system $O-XZ$ is established by taking the hip joint as the origin O. The rotation angles of thigh and shank are θ_1 and θ_2,

https://doi.org/10.1017/S0263574722001436 Published online by Cambridge University Press

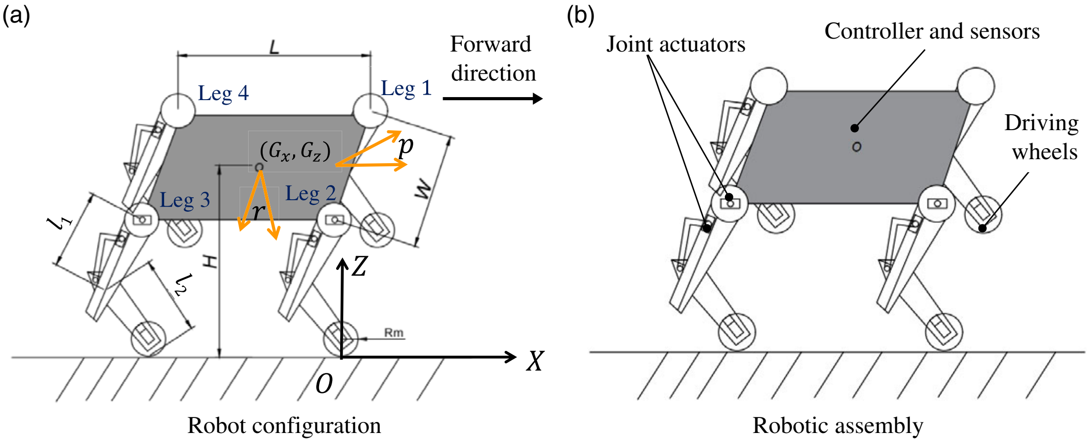

Figure 1. *The model of wheel-legged robot.*

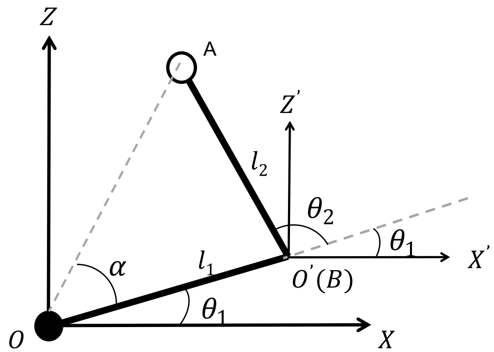

Figure 2. *The single-leg structure of the wheel-legged robot.*

respectively. The coordinates of the end effector of foot are (x_A, z_A). An auxiliary coordinate system $O' - X'Z'$ is established by taking the knee joint as the origin O'. As thus, the position coordinates of end effector of foot in the auxiliary coordinate system is (x'_A, z'_A).

3.1.1. Inverse solution of foot position

The problem of the inverse solution of the foot position of the wheel-legged robot can be described as: the problem of solving the rotation angles of θ_1 and θ_2 when the coordinates of end effector of foot (x_A, z_A) and the length of l_1 and l_2 are known. According to the geometric relationship, the following results can be obtained as:

$$\begin{cases} \theta_1 = \arctan\left(\dfrac{z_A}{x_A}\right) - \arccos\left(\dfrac{{l_2}^2 - {l_1}^2 - \left({x_A}^2 + {z_A}^2\right)}{-2l_1\sqrt{{x_A}^2 + {z_A}^2}}\right) \\ \theta_2 = \pi - \arccos\left(\dfrac{{x_A}^2 + {z_A}^2 - {l_1}^2 - {l_2}^2}{-2l_1 l_2}\right) \end{cases} \tag{1}$$

3.1.2. Forward solution of foot position

The problem of the forward solution of the foot position of the wheel-legged robot can be described as: the problem of solving the coordinates of end effector of foot (x_A, z_A) when the rotation angles of θ_1 and

θ_2 and the length of l_1 and l_2 are known. According to the geometric relationship, the following results can be obtained as:

$$\begin{cases} x_A = l_1 \cos(\theta_1) - l_2 \cos(\theta_1 + \theta_2) \\ z_A = l_1 \sin(\theta_1) + l_2 \sin(\theta_1 + \theta_2) \end{cases} \tag{2}$$

3.1.3. Trajectory planning of foot

The cycloid method is employed to generate the trajectory of foot. Define (x_s, z_s) and (x_f, z_f) as the start and end point position of the foot/cycloid, respectively. Define T, h, and λ as the cycle, height, and duty ratio of step. Then, the trajectory planning of foot can be obtained as:

$$\begin{cases} x_{\exp} = (x_f - x_s)\dfrac{\sigma - \sin\sigma}{2\pi} + x_s \\ z_{\exp} = h\left(\dfrac{1 - \cos\sigma}{2}\right) + z_s \\ \sigma = \dfrac{2\pi t}{\lambda T} \end{cases} \tag{3}$$

Specially, λT is the time period in the swing phase and $(1 - \lambda)T$ is the time period in the support phase.

3.2. Wheeled motion model

Considering the wheeled motion of the wheel-legged robot as the plane motion of a rigid body, the whole movement can be decomposed into the combining motion of rotation and translation of the robot. The differential wheeled motion model of the wheel-legged robot is shown in Fig. 3, where the velocity, angular velocity, and rotation radius of robot around the center of rotation O_c are V_c, ω_c, and R_c, respectively. The velocities, angular velocities, and rotation radiuses of four driving wheels around the center of rotation O_c are $V_1 \sim V_4$, $\omega_1 \sim \omega_4$, and $R_1 \sim R_4$, respectively. The velocities, angular velocities, and rotation radiuses of four driving wheels velocities around their rolling shafts are $V_{1y} \sim V_{4y}$, $\omega_{m1} \sim \omega_{m4}$, and $R_{m1} \sim R_{m4}$, respectively. The fixed wheelbases between front and hind, left and right are D_1 and D_2, respectively. Noting that the velocities V_i can be decomposed into the forward velocities V_{iy} and the lateral velocities V_{ix}, where V_{iy} and V_{ix} are the partial speeds generated by the rolling and sliding friction, respectively.

3.2.1. Inverse solution of centroid velocity

The problem of inverse solution of the wheel-legged robot in the wheeled motion can be described as: the problem of solving the forward component velocities of the four driving wheels around their rolling shafts $V_{1y} \sim V_{4y}$ when the velocity V_c and angular velocity ω_c of robot around the center of rotation O_c are known.

The angular velocity of the rigid-body motion is satisfied as:

$$\omega_c = \frac{V_c}{R_c} = \omega_1 = \omega_2 = \omega_3 = \omega_4 \tag{4}$$

In order to determine R_c, the four-wheel differential motion model in Fig. 3 is equivalent to a two-wheel differential motion model, as shown in Fig. 4, where, V_l represents the resultant forward speed of the left No. 1 and No. 4 driving wheels, V_r represents the resultant forward speed of the right No. 2 and No. 3 driving wheels, V_f represents the resultant lateral speed of the front No. 1 and No. 2 driving wheels, and V_b represents the resultant lateral speed of the hind No. 3 and No. 4 drive wheels.

https://doi.org/10.1017/S0263574722001436 Published online by Cambridge University Press

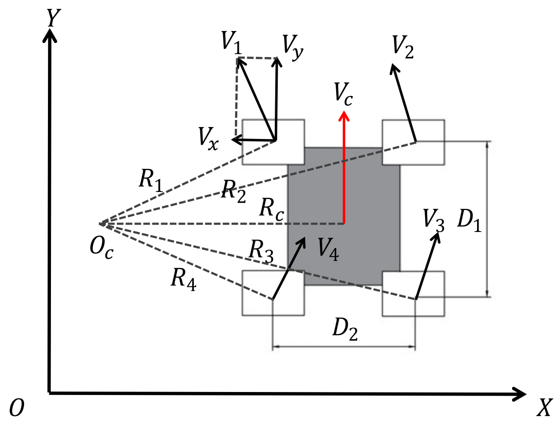

Figure 3. *Four-wheel differential motion model.*

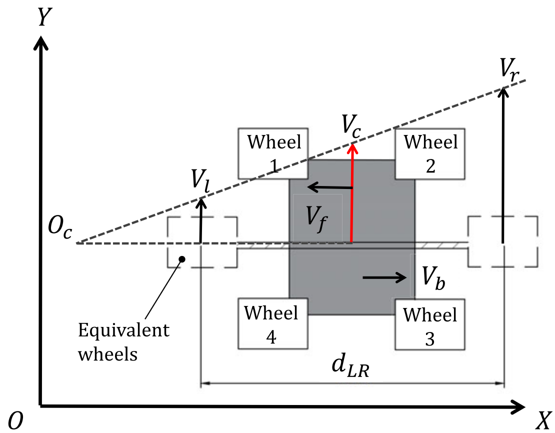

Figure 4. *Equivalent two-wheel differential motion model.*

Use two-wheel differential motion model to obtain the motion law of centroid velocity as:

$$R_c = \frac{V_c}{\omega_c} = \frac{(V_l + V_r)d_{LR}}{2(V_r - V_l)}$$
$$\begin{bmatrix} V_r \\ V_l \end{bmatrix} = \begin{bmatrix} V_c + \dfrac{d_{LR}}{2}\omega_c \\ V_c - \dfrac{d_{LR}}{2}\omega_c \end{bmatrix} \tag{5}$$

where d_{LR} is the virtual wheelbase of the equivalent two-wheel differential motion model, and its equivalent result is related to the robot load, the relative friction coefficient between the tire and the ground, the turning radius and the position of the center of mass, which is usually determined by repeated test fitting in a certain environment.

Then, the forward velocities of the four driving wheels around their rolling shafts are as follows:

$$\begin{cases} V_{1y} = V_{4y} = V_l \\ V_{2y} = V_{3y} = V_r \\ V_{1x} = V_{2x} = V_f \\ V_{3x} = V_{4x} = V_b \end{cases} \tag{6}$$

https://doi.org/10.1017/S0263574722001436 Published online by Cambridge University Press

3.2.2. Forward solution of centroid velocity

The problem of forward solution of the wheel-legged robot in the wheeled motion can be described as: the problem of solving the velocity V_c and angular velocity ω_c of robot around the center of rotation O_c when the forward component velocities of the four driving wheels around their rolling shafts $V_{1y} \sim V_{4y}$ are known.

According to the two-wheel differential motion model, the results can be obtained as follows.

$$\begin{bmatrix} V_c \\ \omega_c \end{bmatrix} = \begin{bmatrix} \dfrac{V_r + V_l}{2} \\ \dfrac{V_r - V_l}{d_{LR}} \end{bmatrix} \tag{7}$$

$$\begin{cases} V_l = V_{1y} = V_{4y} \\ V_r = V_{2y} = V_{3y} \end{cases} \tag{8}$$

Assume that the speeds of left two wheels are the same and the speeds of right two wheels are the same, it yields

$$\begin{cases} V_l = \omega_{m1} R_{m1} = \omega_{m4} R_{m4} \\ V_r = \omega_{m2} R_{m2} = \omega_{m3} R_{m3} \end{cases} \tag{9}$$

where

$$\begin{cases} R_{m1} = R_{m2} = R_{m3} = R_{m4} \\ \omega_{m1} = \omega_{m4} \\ \omega_{m2} = \omega_{m3} \end{cases} \tag{10}$$

4. Controller of wheel-legged robot

As shown in Fig. 5, the wheel-legged robot owns three motion modal: legged motion, wheeled motion, and cooperation motion of legs and wheels. The robot should be able to choose which motion modal to use according to the terrain and environment that it is located. The terrain and environment can be sampled by environment perception system. For simplicity, only attitude message of robot is considered here. For legged motion, there are many gaits such as walk, trot, bound, and gallop. The gait planning focuses on two common gaits: walk and trot. For wheeled motion, the classical differential control algorithm is utilized. The cooperation motion of legs and wheels are addressed by integrating the legged and wheeled motion and considering attitude balance simultaneously. Among them, the method of quaternion is used to solve the attitude sensor data. Compared with other methods, the method of quaternion has the advantages of fast speed, high efficiency, and no universal lock problem in Euler angle calculation. On this basis, processing the solution results with complementary filtering can make up for the limitations of the attitude sensor gyroscope and accelerometer itself [19]. Finally, the Proportional-Integral-Derivative (PID) controller is used to achieve the stability of attitude balance control.

4.1. Attitude calculation and sensor data fusion

As the closed-loop feedback, the data returned by the attitude sensor should be calculated first to obtain a stable and accurate attitude result. The return values of the attitude sensor are the gyroscope data $\{g_x, g_y, g_z\}$ and the accelerometer data $\{a_x, a_y, a_z\}$, respectively, where the gyroscope data unit is rad/s. The quaternion method is employed to obtain two attitude angles: pitch p and roll r.

Build a quaternion

$$q_0 + q_1 i + q_2 j + q_3 k \tag{11}$$

https://doi.org/10.1017/S0263574722001436 Published online by Cambridge University Press

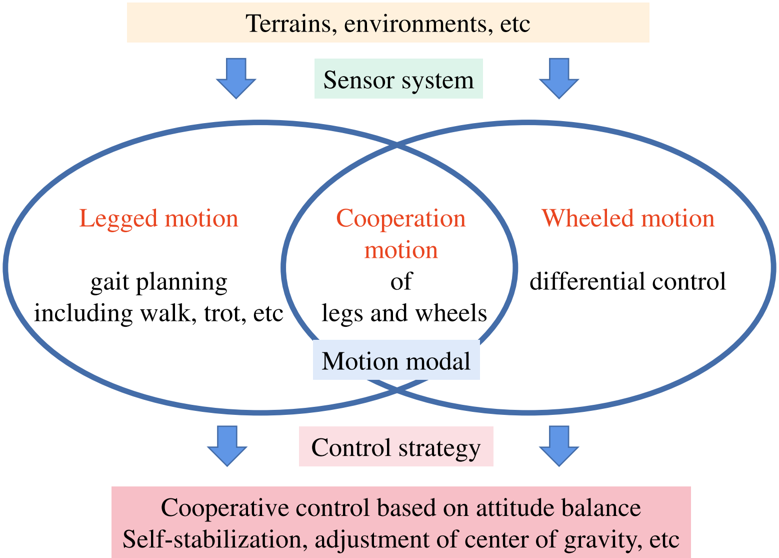

Figure 5. *Control strategy of the wheel-legged robot.*

and solve the quaternion by using the gyroscope data $\{g_x, g_y, g_z\}$ of the attitude sensor:

$$\begin{bmatrix} q_0 \\ q_1 \\ q_2 \\ q_3 \end{bmatrix}_{t+\Delta t} = \begin{bmatrix} q_0 \\ q_1 \\ q_2 \\ q_3 \end{bmatrix}_t + \frac{\Delta t}{2} \begin{bmatrix} -g_x q_1 - g_y q_2 - g_z q_3 \\ g_x q_0 - g_y q_3 + g_z q_2 \\ g_x q_3 + g_y q_0 - g_z q_1 \\ -g_x q_2 + g_y q_1 + g_z q_0 \end{bmatrix} \tag{12}$$

where Δt is the sampling time.

According to the relationship between quaternion and Euler angles [20], it yields

$$\begin{cases} p = -\arcsin\left(2(q_1 q_3 - q_0 q_2)\right) \\ r = \arctan\left(\dfrac{2(q_2 q_3 + q_0 q_1)}{{q_0}^2 - {q_1}^2 - {q_2}^2 + {q_3}^2}\right) \end{cases} \tag{13}$$

Since the raw data of the gyroscope has accumulated error drift, it is considered to be compensated by combining the data of the accelerometer. At the same time, the raw data of the accelerometer has high-frequency jumps, and the two can be complementary and fused.

The method of Mahony [21] is used to process and estimate the theoretical gravitational acceleration by using the angular velocity as follows:

$$\begin{cases} v_x = 2(q_1 q_3 - q_0 q_2) \\ v_y = 2(q_0 q_1 + q_2 q_3) \\ v_z = {q_0}^2 - {q_1}^2 - {q_2}^2 + {q_3}^2 \end{cases} \tag{14}$$

The error of gyroscope measurements can be described by using the cross-product of the estimated gravitational acceleration $\{v_x, v_y, v_z\}$ and the accelerometer data as follows:

$$\begin{cases} e_x = a_y v_z - a_z v_y \\ e_y = a_z v_x - a_x v_z \\ e_z = a_x v_y - a_y v_x \end{cases} \tag{15}$$

https://doi.org/10.1017/S0263574722001436 Published online by Cambridge University Press

Finally, use the error to perform PID control on the data of the gyroscope, which can compensate the original gyroscope data:

$$\begin{cases} \Delta g_x = k_p e_x + k_i \int e_x \\ \Delta g_y = k_p e_y + k_i \int e_y \\ \Delta g_z = k_p e_z + k_i \int e_z \end{cases} \tag{16}$$

Use the data in Eq. (16) to obtain the quaternion again, and then the attitude angles p and r can be solved.

4.2. Attitude stability control

4.2.1. Adjustment of center of gravity

Attitude stability control is to keep the attitude of robot body balance and adjust the center of gravity of robot inside the static or dynamic stability margin when the robot goes through complex terrains and environments including slopes, stairs, rough grounds, obstacles culverts, etc. For example, the attitude can be kept balance when $p = 0$ and $r = 0$.

According to the relationship between the change of attitude angles p and r and the desired position of the center of gravity, using p control yields

$$\begin{cases} G_x = G_{x\_\exp} + \rho H \tan(\Delta p) \\ G_z = G_{z\_\exp} \end{cases} \tag{17}$$

where $(G_{x\_\exp}, G_{z\_\exp})$ is the desired position of center of gravity, (G_x, G_z) is the real position of center of gravity, Δp is the change value of the pitch angle, and ρ is the gain coefficient which can be self-defined.

In the process of adjusting the attitude angle and the center of gravity, PID control algorithm is used for both. Being able to adjust the center of gravity is the basis for achieving attitude balance. In the subsequent analysis of different gait in the legged motion, the position of the center of gravity and the attitude angle will be adjusted to prevent the robot from slipping or falling so that the robot can be stable in different motion modal.

4.2.2. Attitude balance

Attitude balance is manifested as the change of attitude balance parameters on the wheel-legged robot, namely pitch angle p and roll angle r. To essence of ensuring attitude balance is to ensure that the attitude angles are unchanged or change according to the expected values. The corresponding relationship between the attitude angle change and the position of the center of gravity has been given above. Thus, as long as the corresponding relationship between the position of the center of gravity and the coordinates of the end effector of foot is known, the attitude balance can be achieved via the inverse solution of foot position. That is, changing the height of different legs can adjust the attitude of the robot body.

Firstly, the increment of the attitude angle is controlled by a PID controller as follows:

$$\begin{cases} p = p_{\exp} - \Delta p k_p - g_x k_d \\ r = r_{\exp} - \Delta r k_p - g_y k_d \end{cases} \tag{18}$$

where $(p_{\exp}, r_{\exp})$ are the desired attitude angles and (g_x, g_y) are the angular accelerations of attitude.

According to the relationship between the position of the center of gravity (G_x, G_y) and the coordinates of the end effector of foot, it yields

$$\begin{cases} x = x_0 + \dfrac{L}{2}(1 - \cos p) - G_x \\ z = z_0 - \dfrac{W}{2} \sin r - \dfrac{L}{2} \cos r \sin p - G_z \end{cases} \tag{19}$$

https://doi.org/10.1017/S0263574722001436 Published online by Cambridge University Press

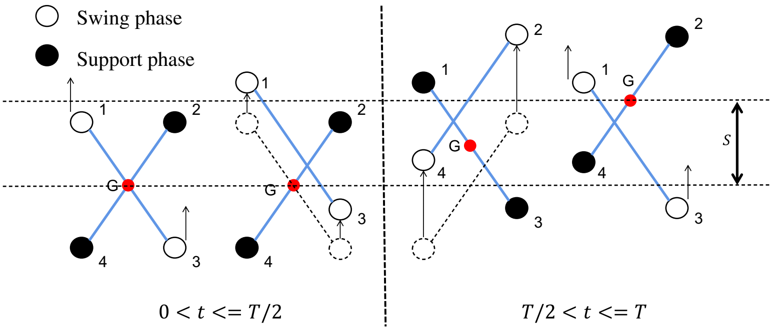

Figure 6. *The changes of trot gait phase sequence and center of gravity.*

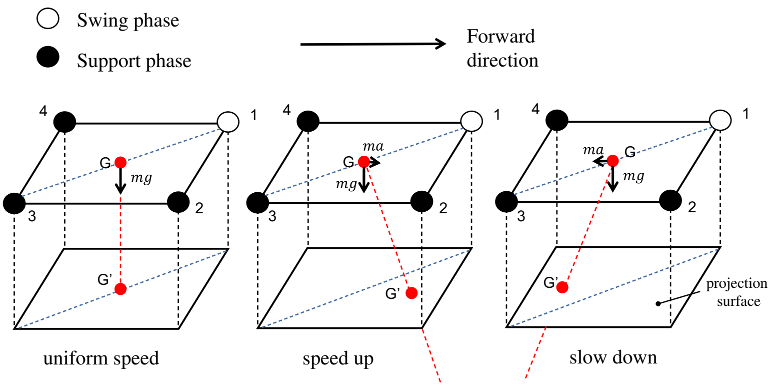

Figure 7. *Actual center of gravity position.*

where (x_0, z_0) are the coordinates of the end effector of foot before the attitude balance adjustment, and (x, z) are the coordinates of the end effector of foot after the attitude balance adjustment. As thus, the attitude balance control of wheel-legged robot is achieved.

4.3. Gait planning of leg motion

The idea of gait planning for the wheel-legged robot is to: (1) design the phase sequence of the legs according to bionics, (2) compensate the center of gravity of the robot under different supports, and (3) adjust the attitude in time to prevent slipping or falling.

4.3.1. Trot gait

The trot gait is a diagonal gait, that is, during a gait cycle T, legs 1 and 3 are in the swing phase and legs 2 and 4 are in the stance phase when $0 < t \le T/2$; legs 1 and 3 are in the stance phase and legs 2 and 4 are in the swing phase when $T/2 < t \le T$.

The changes of trot gait phase sequence and the center of gravity G in one cycle are shown in Fig. 6, where the step length is S.

It can be seen that in order to ensure the stability of the robot, the center of gravity of the robot should fall on the diagonal of the support legs. As shown in Fig. 7, if the projection of the center of gravity is not on the diagonal, the robot will tip over or roll over. However, if the gait sequence is simply carried out, only the influence of the gravity of robot body is taken into account. In fact, the projected position of the center of gravity of robot body is related to the resultant force of gravity and inertial force. Whether the robot accelerates and decelerates or not does matter.

https://doi.org/10.1017/S0263574722001436 Published online by Cambridge University Press

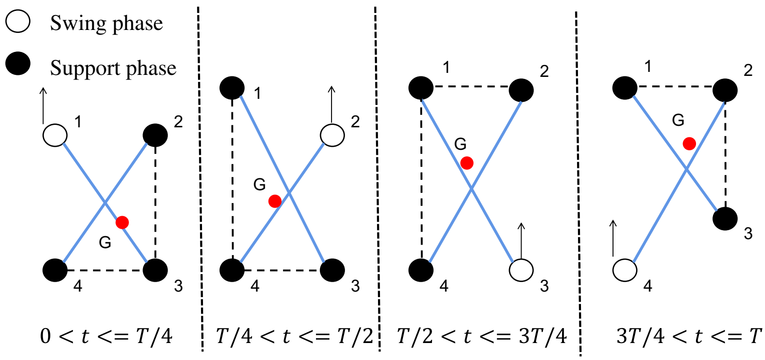

Figure 8. *The changes of walk gait phase sequence and center of gravity.*

In order to compensate for the influence of the center of gravity offset on the stability of the robot, there are two ways: one is to adjust the leg when stepping forward, that is, to adjust the final projected position of center of gravity in advance by adjusting the stride S; the other is to adjust the attitude after landing, that is, to adjust the projected position of center of gravity moving to the diagonal of the support legs. These two ways are both used to make the trot movement more stable in the whole step cycle.

According to the attitude angles p and r, and the influence of the stride S on the projected position of the center of gravity, the adjustment value of each stride can be calculated as;

$$\begin{cases} \Delta G_x = S - \dfrac{L}{2}(1 - \cos(p)) \\ \Delta G_z = \dfrac{W}{2}\sin(r) + \dfrac{L}{2}\cos(r)\sin(p) \end{cases} \tag{20}$$

4.3.2. Walk gait

The walk gait is a triangular gait, that is, at any time, three legs are in the support phase and one leg is in the swing phase. The changes of walk gait phase sequence and the center of gravity G in one cycle are shown in Fig. 8,

It can be seen that the condition for the stability of the center of gravity under the walk gait is that the projection position of the resultant force of gravity and inertial force should fall within the triangular plane formed by the three support legs at any time; otherwise, the robot will fall or roll over. Considering that the speed of the walk gait is much lower than that of the trot gait, the center of gravity is adjusted before the leg swing.

Assume that the phase sequence of the legs is fixed, the idea of adjusting the center of gravity is to: (1) in the first stage, move the center of gravity of robot backward to a position with sufficient margin before legs 1 and 2 stepping forward; (2) in the second stage, move the center of gravity of robot forward to a position with sufficient margin before legs 3 and 4 stepping forward; and (3) in the third stage, after completing a four-legged gait cycle, move the center of gravity backward to the initial position. The method of adjusting the center of gravity is shown in Fig. 9.

In the first stage, the center of gravity is adjusted as:

$$G_x = G_{x0} - S_{back} \tag{21}$$

In the second stage, the center of gravity is adjusted as:

$$G_x = G_{x0} + S_{forward} \tag{22}$$

In the third stage, the center of gravity is adjusted as:

$$G_x = G_{x0} \tag{23}$$

https://doi.org/10.1017/S0263574722001436 Published online by Cambridge University Press

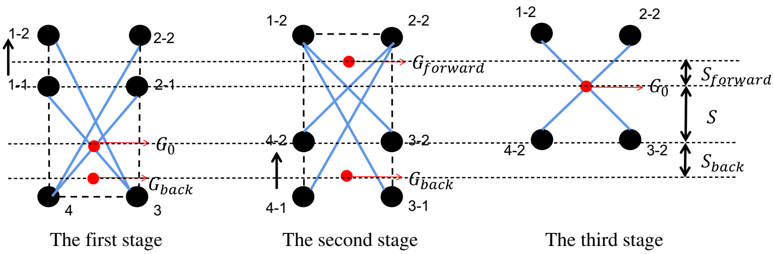

Figure 9. *Adjusting the center of gravity in three stages.*

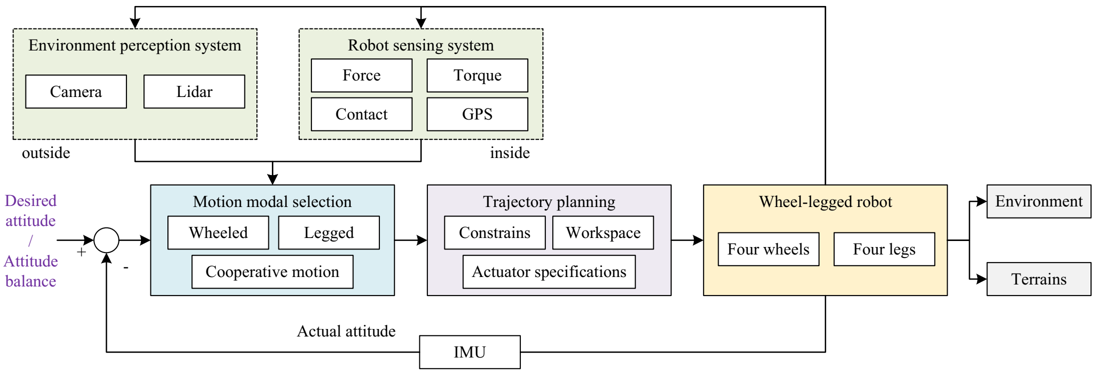

Figure 10. *Cooperative motion controller.*

where G_{x0} is the initial position of the center of gravity of robot, and S_{back} and $S_{forward}$ are the adjustment margins, which can be determined by trials.

4.4. Differential control of wheeled motion

Differential control of wheeled motion can be used to achieve the forward and steering control of robot. With $[V_c, \omega_c]$ are known, based on the inverse solution of the above equivalent two-wheel differential motion model, the output of control speed $\{n_1, n_2, n_3, n_4\}$ of the four driving wheels can be obtained as:

$$n_i = \frac{V_{iy}}{2\pi R_{mi}} (i = 1, 2, 3, 4) \tag{24}$$

4.5. Cooperative motion control of wheels and legs

4.5.1. Cooperative motion controller

After investigating the kinematics, the attitude stability control, the gait planning of leg motion, and the differential control of wheeled motion of wheel-legged robot, the cooperative motion control of wheels and legs can be further addressed. Combining the above four issues, the cooperative motion controller can be designed as shown in Fig. 10. There are three closed loops in the controller, and the corresponding desired inputs are desired center of gravity, desired attitude angles, and body speed. The actual center of gravity is calculated by the foot positions of support legs, and the actual attitude angles and body speed are calculated by the IMU data. And there are three PID controllers are used to track their desired values without considering their couplings with each other. Through the inverse solution of foot position and centroid velocity, the generated 12 control laws for 8 joint actuators and 4 driving wheels can achieve the cooperative motion of whole body of wheel-legged robot including body, wheels, and legs.

Table I. *Comparison of walk gait and trot gait parameters.*

Gait	Speed	Foot numbers in support phase	Stability margin	Stride	Leg lift
Trot	Fast	2	Insufficient (dynamic)	Long	Low
Walk	Slow	3	Sufficient (static)	Short	High

4.5.2. Cooperative control strategy

The cooperative control strategy of wheel-legged robot also integrates the control strategy of wheeled and legged robot. Cooperative motion control of wheels and legs can be utilized to handle different terrains and environments.

For different terrains, it can be summarized as follows:

- For even terrains, such as plain grounds and slopes, wheeled motion is enough.
- For continuous terrains and discontinuous terrains the wheel can turn over, wheeled motion is enough, and legged motion can be employed to keep the attitude balance.
- For uneven terrains and discontinuous terrains, the wheel cannot turn over, such as stairs, legged motion is essential, and cooperative motion of wheels and legs would be better for speed, efficiency, and stability.

In sum, wheeled motion is the first choice for movement since of its high speed, efficiency and stability, and low vibration. For easy terrains, only wheeled motion is necessary. For moderately difficult terrains, legged motion cooperates with wheeled motion to achieve stable attitude of robot body. For moderately difficult terrains, wheeled motion cooperates with legged motion to improve the speed of legged locomotion.

For different environments, it can be summarized as follows:

- For the culvert environments, the wheel-legged robot can lower the center of mass of robot by legged motion and go through the culvert by wheeled motion.
- For some obstacle environments, the wheel-legged robot can higher the center of mass of robot by legged motion and go across over the obstacle by wheeled motion.
- For one-side slope environments, the wheel-legged robot can use the legged motion to adjust the attitude of body and use the wheeled motion to move forward.

In sum, the cooperative motion control of wheels and legs can greatly improve the environmental adaptivity and reliability via the motion redundancy between wheeled and legged motion. The motion modal selection is case-dependent based on terrains and environments.

4.5.3. Wheel-legged cooperation

In real applications, for structured terrains, preplanned motion trajectory can work well by involving some small adjustments. For unstructured terrains, the real-time motion control of whole body is required for stable movement. Therefore, the environment perception system for robot should be set up first to sense the terrains. For simplicity, the terrains are assumed to be known.

As mentioned above, legged motion includes walk and trot gait. The walk and trot gait parameters are compared in Table I. Through the analysis of trot gait and walk gait, it can be concluded that walk gait has stronger obstacle-crossing ability. The reason is that there are only two legs are in stance phase in trot gait at the same time even if the trot gait is fast, resulting in a small stability margin of the center of gravity, as shown in Fig. 11(a), so that the stride or leg lift can not be too large. On the contrary, even though the frequency of walk gait is low and there are three support legs at the same time, the walk gait has a larger stability margin of the center of gravity, as shown in Fig. 11(b), so that it can have a larger stride or leg lift. Thus, the walk gait owns a stronger obstacle-crossing ability, and it is mainly employed

https://doi.org/10.1017/S0263574722001436 Published online by Cambridge University Press

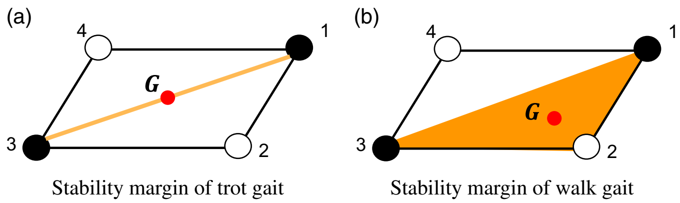

Figure 11. *Comparison of stability margin of center of gravity.*

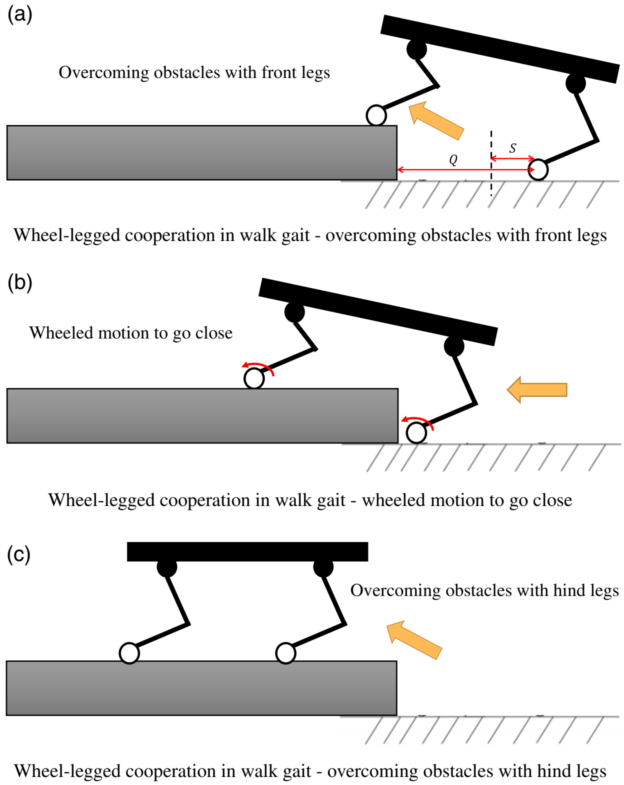

Figure 12. *The process of wheel-legged cooperation for climbing stairs.*

to do the cooperative control of wheels and legs. Of course, the wheel-legged cooperation with four support legs will have the best stability, but it have to lift off one or more leg to overcome obstacles.

In order to make up for the lack of low frequency of walk gait, wheeled motion can be added into the gait. Under the premise of adjusting the center of gravity to be stable, the walk gait combining wheeled motion can overcome obstacles more quickly and validate the efficiency of wheel-legged cooperation. More concretely, the cooperative control of wheels and legs for climbing stairs will be given out detailedly in the following, and its stability will be analyzed.

The process of wheel-legged cooperation for climbing stairs is shown in Fig. 12, where Q is the distance between the feet of hind legs and the edge of stair. If $S < Q$, that is, the robot cannot cross up the stair within one step, then the time for stair climbing will be lager that T. Therefore, there are three steps in the wheel-legged cooperation to shorten the climbing time. The first step is approaching the stairs by means of wheeled motion, and then using legged motion to make the front legs lift up the stairs, as shown in Fig. 12(a). The second step is using the wheeled motion to go on moving forward so that the hind legs go close to the stair edge, as shown in Fig. 12(b). The third step is using legged motion to make the hind legs lift up the stairs as well, as shown in Fig. 12(c). In this way, it can be ensured that the goal of crossing stairs can be achieved within one cycle of walk gait, and thereby the obstacle-crossing efficiency of robot can be greatly improved. Noting that the three steps can be performed individually, or two adjacent steps can be executed simultaneously.

4.5.4. Cooperative stability analysis of wheel-legged motion

The purpose of the stability analysis of the cooperative control of the wheel-legged is to ensure that the wheel-legged robot will not fall and other unstable phenomenons according to the different steps of wheel-legged cooperation. Based on the three steps discussed above, the stability adjustment of wheel-legged cooperation with walk gait will be further studied in the following.

(1) Overcoming obstacles with front legs

According to the characteristics of walk gait, it essential to ensure that the center of gravity falls in the triangle formed by the three legs in stance phase. Therefore, before overcoming the obstacle by using front legs 1 and 2, the first point is to adjust the center of gravity into the stable area of the triangle formed by legs 2, 3, and 4 to legs 1, 3, and 4, as shown in Fig. 13(a) and (b). That is, adjust the center of gravity of the robot backward to a position with sufficient margin according to the first step of walk gait.

As shown in Fig. 13(c), there exists a stability margin of center of gravity δ, which is required to meet

$$\delta_{\min} < \delta < \delta_{\max} \tag{25}$$

where $\delta_{\min}$ and $\delta_{\max}$ are the lower and upper bound of stability margin of center of gravity δ, respectively. If $\delta < \delta_{\min}$, then the robot will fall forward. If $\delta > \delta_{\max}$, then the robot will fall backward.

If the distance between front and hind legs L and the coordinates of foot end effector (x_A, y_A) are known, then it yields

$$\begin{aligned} \delta_{\min} &= 0 \\ \delta_{\max} &= \delta_{\min} + \frac{L}{2} - |x_A| \end{aligned} \tag{26}$$

Then, the adjustment of center of gravity can be obtained as:

$$\begin{cases} G_x = G_{x0} + S_{back} \\ 0 < S_{back} < \delta_{\max} - \delta_{\min} \end{cases} \tag{27}$$

(2) Wheeled motion to go close

In the second process of wheel-legged robot using wheeled motion to go close, since the four legs are all in stance phase, the lower and upper bound of stability margin of center of gravity will change as:

$$\delta_{\min} = -\frac{L}{2} \tag{28}$$

Thus, the center of gravity can be kept still to for stable wheeled motion.

(3) Overcoming obstacles with hind legs

Before overcoming the obstacle by using hind legs 3 and 4, the first point is to adjust the center of gravity into the stable area of the triangle formed by legs 1, 2, and 4 to legs 1, 2, and 3, as shown in Fig. 13(b). That is, adjust the center of gravity of the robot forward to a position with sufficient margin according to the second step of walk gait.

As shown in Fig. 13(d), the stability margin of center of gravity δ is required to meet

$$\delta'_{\min} < \delta < \delta'_{\max} \tag{29}$$

https://doi.org/10.1017/S0263574722001436 Published online by Cambridge University Press

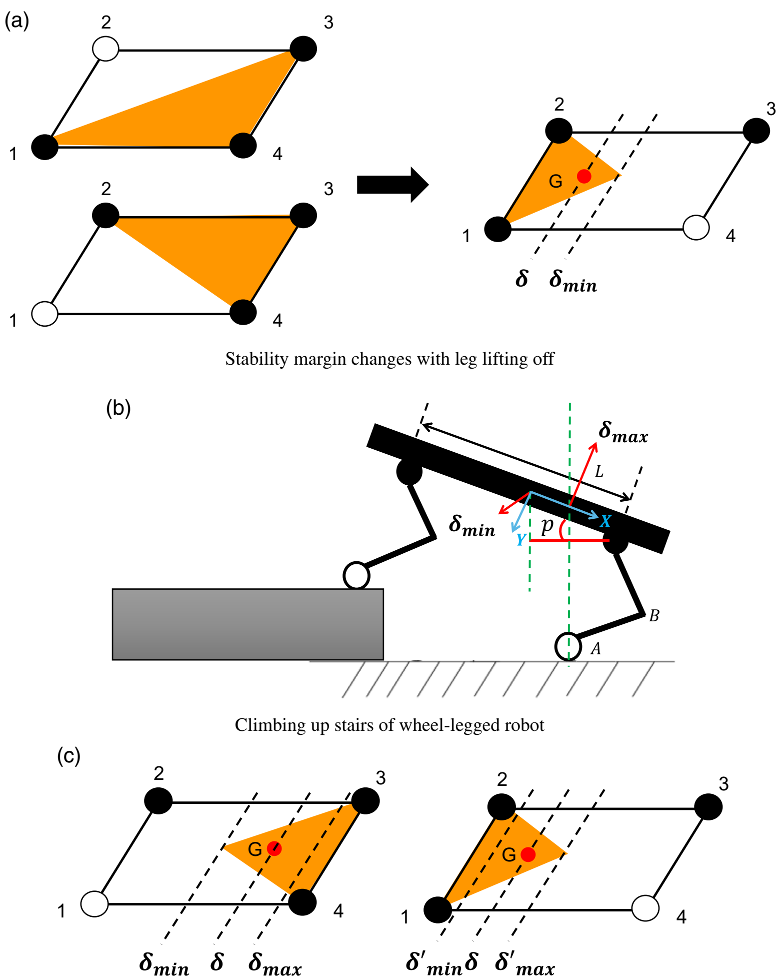

Stability margin changes with leg lifting off

Climbing up stairs of wheel-legged robot

Stability margin of robot overcoming obstacles with front legs

Stability margin of robot overcoming obstacles with hind legs

Figure 13. *Stability analysis of overcoming obstacles.*

where $\delta'_{\min}$ and $\delta'_{\max}$ are another lower and upper bound of stability margin of center of gravity δ, respectively. If $\delta < \delta'_{\min}$, then the robot will fall forward. If $\delta > \delta'_{\max}$, then the robot will fall backward.

If the distance between front and hind legs L and the coordinates of foot end effector (x_A, y_A) are known, then it yields

$$\begin{aligned} \delta_{\min} &= \delta_{\max} - \frac{L}{2} - |x_A| \\ \delta_{\max} &= 0 \end{aligned} \tag{30}$$

Then, the adjustment of center of gravity can be obtained as:

$$\begin{cases} G_x = G_{x0} - S_{forward} \\ 0 < S_{forward} < \delta'_{\max} - \delta'_{\min} \end{cases} \tag{31}$$

As thus, the wheel-legged cooperation will be stability-guaranteed.

https://doi.org/10.1017/S0263574722001436 Published online by Cambridge University Press

Table II. Comparison of walk gait and trot gait parameters.

Initial height of center of gravity H_{CoG}	**110 mm**
Length of body L	142 mm
Width of body W	108 mm
Length of thigh l_1	80 mm
Length of shank l_2	62 mm
Length of step S	32 mm
Height of step H	30 mm
Cycle of step T	1.5 s
Weight of robot m	1.3 kg

Figure 14. *Three motion modal of wheel-legged robot.*

5. Experimental validations

To validate the proposed method, a desktop-level wheel-legged robot prototype is established and some experiments are implemented on different terrains and environments.

5.1. Hardware platform

The wheel-legged robot has four legs with four wheels on each end effector of foot of leg and each leg has two DoFs. The wheel is actuated by DC motor, and the joint of leg is actuated by steering engine. The robot body is formed by 3D printing and there is a microcontroller (STM32F427II) and a IMU/gyroscope (MPU6500) mounting on the body to control the wheels and legs and monitor the attitude angles of body, respectively. STM32F427 carries on the UCOS-III operating system to meet the needs of synchronous multiplexing of computing. The system parameters of wheel-legged robot is shown in Table II.

(a)

Going through a culvert

(b)

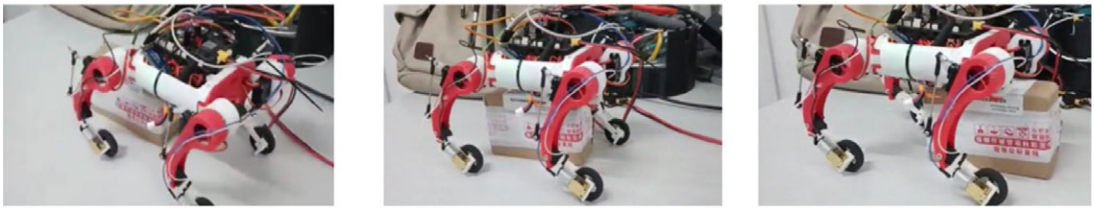

Going cross over an obstacle

(c)

Going across an one-side slope

Figure 15. *Overcoming complex environments of wheel-legged robot.*

5.2. Experiments

As shown in Fig. 14, the experiments validate the ability of three motion modal of robot: legged motion, wheeled motion, and wheel-legged cooperation. It is easy to find that the robot can walk, trot, and wheeled travel on the plain ground in Fig. 14(a), (b), and (c), respectively. And the wheeled motion is with the fastest moving speed, while the walk gait is with the lowest moving speed. In Fig. 14(d), the robot can go up and down the stairs with wheel-legged cooperation.

As shown in Fig. 15, the experiments validate the ability of overcoming complex environments of robot, including handling culvert, obstacle and one-side slope, etc., by using the cooperative motion control of wheels and legs. It is easy to find that the robot can go through a culvert, going cross over an obstacle and going across an one-side slope in Fig. 15(a), (b), and (c), respectively. The mode of travel over complex environments has more stable attitude and less vibration than that with leg lifting off the ground.

5.3. Result analysis

In the experiments, the gait and the center of gravity are monitored. The measurement results are shown in Fig. 16. The trajectory of end effector of foot and the trajectory of center of gravity of trot gait on plain ground are shown in Fig. 16(a) and (b), respectively. It can be seen that the center of gravity of robot can be kept around the fixed theoretical value without large change in the horizonal and vertical direction under the gait parameters in Table II. The trajectory of end effector of foot and the trajectory of center of gravity of trot gait on plain ground are shown in Fig. 16(c) and (d), respectively. It can be seen that the center of gravity of robot can be kept around the fixed theoretical value of height, and the robot

https://doi.org/10.1017/S0263574722001436 Published online by Cambridge University Press

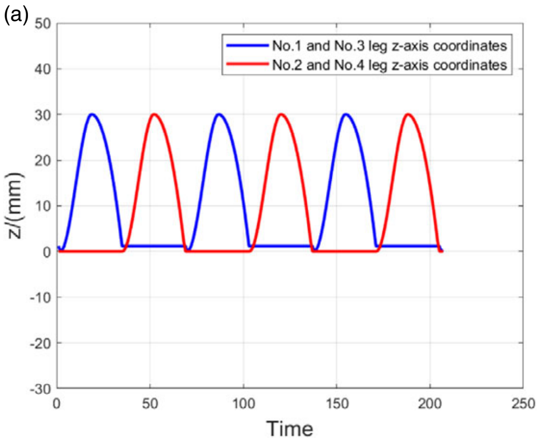

The trajectory of end effector of foot of trot gait on plain ground

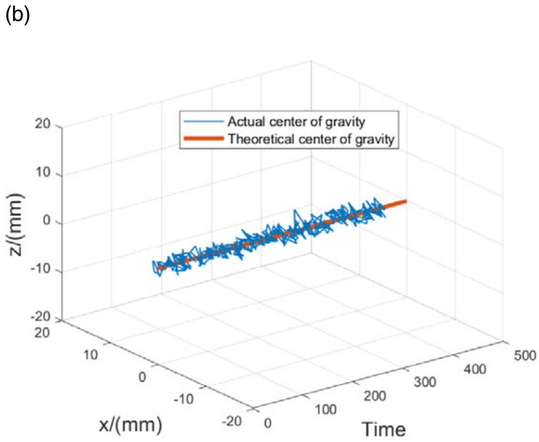

The trajectory of center of gravity of trot gait on plain ground

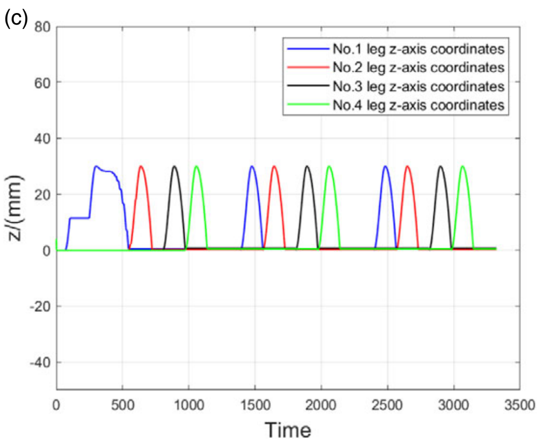

The trajectory of end effector of foot of walk gait on plain ground

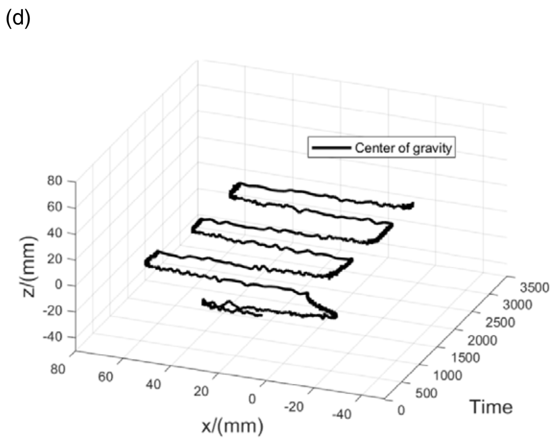

The trajectory of center of gravity of walk gait on plain ground

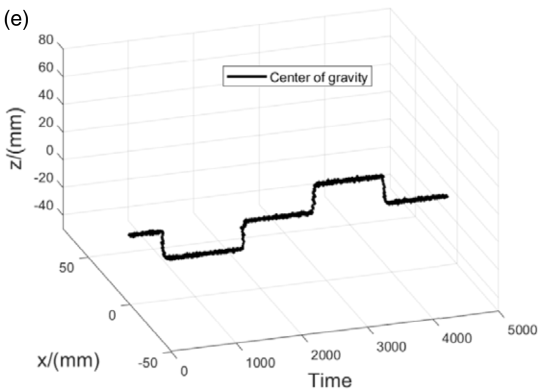

The trajectory of center of gravity of wheel-legged cooperation for going through a culvert and cross over an obstacle

Figure 16. *Trajectory of gait and the center of gravity.*

https://doi.org/10.1017/S0263574722001436 Published online by Cambridge University Press

Table III. *Comparison of walk gait and trot gait parameters.*

Fastest speed	**1.1 m/s**
Height of climbing step	26 mm
Angle of climbing slope	31°
Height of culvert to go through	90 mm
Height of obstacle to go cross over	140 mm

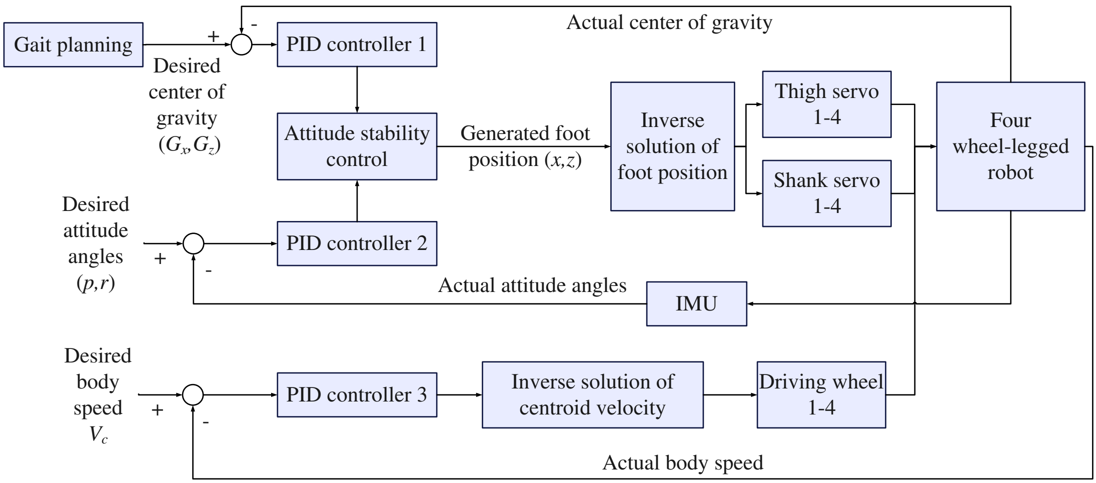

Figure 17. *Control scheme of wheel-legged robot.*

will move back and forth periodically under the gait parameters in Table II. The trajectory of center of gravity of wheel-legged cooperation for going through a culvert and cross over an obstacle is shown in Fig. 16(e). It can be seen that the center of gravity of robot can change with the experimental limitation to improve the traversability.

Through many trials, the motion performance of wheel-legged robot can be summarized in Table III.

6. Discussions

The famous quadruped robot, Anymal, developed by ETH Zurich, has three published papers in the journal Science Robotics. The first one article uses the own status data of robot to learn agile and dynamic motor skills for legged robots [17], and the last two articles use both the own status data and external environmental information to learn quadrupedal locomotion over challenging terrain [18] and robust perceptive locomotion for quadrupedal robots in the wild [19]. For reference, there should be a more comprehensive control scheme of wheel-legged robot based on Fig. 17, as shown in Fig. 17, where the upper two dashed blocks can be added into the control to show more information about terrains, environments, and dynamic interactions for robot. And then, more reasonable and optimal actuator policy can be rewarded and learned to enhance the locomotion performance if the required data inside and outside of robot are obtained. Of course, the control objective can be diversified and not limited to the attitude balance, that is, the wheel-legged cooperation can be used to achieve other goals, such as performing tasks.

The wheel-legged cooperation with three and four support legs is studied above. How the robot will behave if there is two support legs, even one? Actually, there are many wheel-legged robots with two support legs including Handle I and II [20], Ascento and Ascento Pro [21], etc. For these robots, both significant performance and dynamic stability can be achieved even if only two legs is in stance phases.

Certainly, the control difficulty will be higher because of the persistent dynamic stability. As so far, the wheel-legged robot with only one support leg is not found yet except for the transient status of wheel-legged robots with more than two support legs.

In the wheel-legged cooperation, the legged motion and wheeled motion can be apart and coupling, corresponding to the intermittent and persistent cooperation, which means wheeled and legged motion will not and will be executed at the same time, respectively. Eventually, the persistent cooperation will behave higher maneuverability. Moreover, the controller in this paper is still simple, and learning-based controller such as reinforcement learning will be a good choice for agile locomotion control [14, 15].

The integration of wheel and leg has two sides. The advantages include that the locomotion performance of wheeled and legged robot can be both extended by wheel-legged cooperation. More motion modal can be selected. The speed, efficiency, stability, and rejection of vibration can be greatly improved. Besides, the control is redundant to avoid faults. The disadvantages include increasing the control inputs and making the control more complicated. Meanwhile, the load capacity of robot will be reduced. In a word, the advantages overweigh the disadvantages. Therefore, the research of wheel-legged robot is meaningful and has a great and far-reaching significance.

7. Conclusions

In this paper, cooperative control strategy of wheel-legged robot based on attitude balance is proposed to integrate the advantages of wheeled and legged motion. The main contributions are concluded as follows:

- The kinematics of wheeled motion and legged motion are given out, and the forward and inverse solutions of both are issued as well. The trajectory planning of foot based on the cycloid method is addressed for the legged motion.
- The controller of wheel-legged robot is designed. Firstly, the attitude angles is calculated, filtered, and fused, and the attitude stability control is realized by moving the center of gravity into stability margin and adjusting the attitude angle to be balance. Secondly, the gait planing of legged motion containing walk and trot gait is studied and compared. Then the walk gait with three stages is chosen to do the cooperation with wheeled motion for more stability. Thirdly, the differential control of wheeled motion is solved as well. Finally, the cooperative motion controller and the cooperative control strategy are proposed based on the above research. The wheel-legged cooperation for climbing stairs is implemented as an example, and the cooperative stability analysis of wheel-legged motion is given out.
- An 8-DOF wheel-legged robot is developed, which has the ability of autonomous attitude control and three motion modal: wheeled, legged, and wheel-legged cooperation. The robot can adjust the gait and center of gravity according to its attitude balance and stability margin to adapt different terrains and environments. The proposed method is validated by experiments with different motion modals, terrains, and environments, and a more comprehensive control scheme considering more inside and outside sensing data is given out, which provide an insight for the locomotion control of wheel-legged robots.

Our future work will focus on developing a larger prototype for possible practical use, and more sensors will be involved in the robot to enhance the mobility further by using some artificial intelligent algorithms.

Author contributions. Guangrong Chen and Sheng Guo conceived and designed the study. Yaojie Shen, Zhaoyang Li, Ningze Wei, Huafeng Lu, and Qingyu Meng conducted data gathering. Yaojie Shen, Zhaoyang Li, Ningze Wei, Huafeng Lu, and Qingyu Meng performed statistical analyses. Yaojie Shen and Guangrong Chen wrote the article.

Financial support. This work was supported by National Natural Science Foundation of China (62103036) and Fundamental Research Funds for the Central Universities (2022JBMC025).

Conflicts of interest. The authors declare no conflicts of interest exist.

Ethical approval. Not applicable.

References

[1] C. Zhang, G. Chen, Z. Li, X. Qiu and S. Guo, "Design and control of a foldable and reconfigurable multi-terrain vehicle with variable wheelbase," *J. Mech. Robot*. **15**(2), 024501 (9 pages) (2022).

[2] G. Chen, N. Wei, J. Li and H. Lu, "Design and Simulation Analysis of A Bionic Ostrich Robot," **In:** *Biomechanics and Modeling in Mechanobiology* (2022) pp. 1–21.

[3] K.-X. Ba, Y.-H. Song, Y.-P. Shi, C.-Y. Wang, G.-L. Ma, Y. Wang, B. Yu and L.-P. Yuan, "A novel one-dimensional force sensor calibration method to improve the contact force solution accuracy for legged robot," *Mech. Mach. Theory* **169**(8), 104685 (2022).

[4] F. Rubio, F. Valero and C. Llopis-Albert, "A review of mobile robots: Concepts, methods, theoretical framework, and applications," *Int. J. Adv. Robot. Syst.* **16**(2), 1729881419839596 (2019).

[5] J. Li, J. Wang, H. Peng, L. Zhang, Y. Hu and H. Su, "Neural fuzzy approximation enhanced autonomous tracking control of the wheel-legged robot under uncertain physical interaction," *Neurocomputing* **410**, 342–353 (2020).

[6] Z. Chen, S. Wang, J. Wang, K. Xu, T. Lei, H. Zhang, X. Wang, D. Liu and J. Si, "Control strategy of stable walking for a hexapod wheel-legged robot," *ISA Trans.* **108**(03), 367–380 (2021).

[7] S. Wang, Z. Chen, J. Li, J. Wang, J. Li and J. Zhao, "Flexible motion framework of the six wheel-legged robot: Experimental results," *IEEE/ASME Trans. Mechatron*. **27**(4), 2246–2257 (2022).

[8] X. Li, H. Zhou, H. Feng, S. Zhang and Y. Fu, "Design and Experiments of A Novel Hydraulic Wheel-Legged Robot (WLR)," **In:** *2018 IEEE/RSJ International Conference on Intelligent Robots and Systems (IROS)* (IEEE, 2018) pp. 3292–3297.

[9] H. Peng, J. Wang, W. Shen and D. Shi, "Cooperative attitude control for a wheel-legged robot," *Peer Peer Netw. Appl.* **12**(6), 1741–1752 (2019).

[10] K. Xu, S. Wang, B. Yue, J. Wang, H. Peng, D. Liu, Z. Chen and M. Shi, "Adaptive impedance control with variable target stiffness for wheel-legged robot on complex unknown terrain," *Mechatronics* **69**(7), 102388 (2020).

[11] L. Ni, L. Wu and H. Zhang, "Parameters uncertainty analysis of posture control of a four-wheel-legged robot with series slow active suspension system," *Mech. Mach. Theory* **175**(1), 104966 (2022).

[12] F. Raza, W. Zhu and M. Hayashibe, "Balance stability augmentation for wheel-legged biped robot through arm acceleration control," *IEEE Access* **9**, 54022–54031 (2021).

[13] S. Wang, L. Cui, J. Zhang, J. Lai, D. Zhang, K. Chen, Y. Zheng, Z. Zhang and Z.-P. Jiang, "Balance Control of A Novel Wheel-Legged Robot: Design and Experiments," **In:** *2021 IEEE International Conference on Robotics and Automation (ICRA)* (IEEE, 2021) pp. 6782–6788.

[14] L. Cui, S. Wang, J. Zhang, D. Zhang, J. Lai, Y. Zheng, Z. Zhang and Z.-P. Jiang, "Learning-based balance control of wheel-legged robots," *IEEE Robot. Automat. Lett*. **6**(4), 7667–7674 (2021).

[15] X. Chen, A. Ghadirzadeh, J. Folkesson, M. Björkman and P. Jensfelt, "Deep Reinforcement Learning to Acquire Navigation Skills for Wheel-Legged Robots in Complex Environments," **In:** *2018 IEEE/RSJ International Conference on Intelligent Robots and Systems (IROS)* (IEEE, 2018) pp. 3110–3116.

[16] K.-X. Ba, Y.-H. Song, C.-Y. Wang, Y.-P. Shi, B. Yu, X. Chen, G.-L. Ma and X.-D. Kong, "A novel kinematics and statics correction algorithm of semi-cylindrical foot end structure for 3-DoF LHDS of legged robots," *Complex Intell. Syst*. **108**(4), 1–21 (2022).

[17] J. Hwangbo, J. Lee, A. Dosovitskiy, D. Bellicoso, V. Tsounis, V. Koltun and M. Hutter, "Learning agile and dynamic motor skills for legged robots," *Sci. Robot*. **4**(26), eaau5872 (2019).

[18] J. Lee, J. Hwangbo, L. Wellhausen, V. Koltun and M. Hutter, "Learning quadrupedal locomotion over challenging terrain," *Sci. Robot*. **5**(47), eabc5986 (2020).

[19] T. Miki, J. Lee, J. Hwangbo, L. Wellhausen, V. Koltun and M. Hutter, "Learning robust perceptive locomotion for quadrupedal robots in the wild," *Sci. Robot*. **7**(62), eabk2822 (2022).

[20] E. Ackerman, "A robot for the worst job in the warehouse: Boston dynamics' stretch can move 800 heavy boxes per hour," *IEEE Spectr*. **59**(1), 50–51 (2022).

[21] V. Klemm, A. Morra, C. Salzmann, F. Tschopp, K. Bodie, L. Gulich, N. Küng, D. Mannhart, C. Pfister, M. Vierneisel, F. Weber, R. Deuber and R. Siegwart, "Ascento: A Two-Wheeled Jumping Robot," **In:** *2019 International Conference on Robotics and Automation (ICRA)* (IEEE, 2019) pp. 7515–7521.

Cite this article: Y. Shen, G. Chen, Z. Li, N. Wei, H. Lu, Q. Meng and S. Guo (2023). "Cooperative control strategy of wheel-legged robot based on attitude balance", Robotica **41**, 566–586. https://doi.org/10.1017/S0263574722001436